Inhibitory role of ginsenoside Rb2 in endothelial senescence and inflammation mediated by microRNA-216a

YUTONG CHEN[1,2*], SHUTING WANG[2*], SHUJUN YANG[2,3], RONGXIA LI[2], YUNYUN YANG[2,4], YU CHEN[2] and WEILI ZHANG[2]

[1]Beijing Institute of Brain Disorders, Laboratory of Brain Disorders, Ministry of Science and Technology, Collaborative Innovation Center for Brain Disorders, Capital Medical University, Beijing 100069; [2]State Key Laboratory of Cardiovascular Disease, Fuwai Hospital, National Center for Cardiovascular Diseases, Peking Union Medical College and Chinese Academy of Medical Sciences, Beijing 100037; [3]Institute of Cardiovascular Diseases, Xiamen Cardiovascular Hospital, Xiamen University, Xiamen, Fujian 361010; [4]Clinical Laboratory of The First Affiliated Hospital of Xiamen University, Xiamen Key Laboratory of Genetic Testing, Xiamen, Fujian 361003, P.R. China

Received July 27, 2020; Accepted March 9, 2021

DOI: 10.3892/mmr.2021.12054

Abstract. Targeting microRNAs (miRs) using small chemical molecules has become a promising strategy for disease treatment. miR-216a has been reported to be a potential therapeutic target in endothelial senescence and atherosclerosis via the Smad3/NF-κB signaling pathway. Ginsenoside Rb2 (Rb2) is the main bioactive component extracted from the plant *Panax ginseng,* and is a widely used traditional Chinese medicine. In the present study, Rb2 was identified to have a high score for miR-216a via bioinformatics analysis based on its sequence and structural features. The microscale thermophoresis experiment further demonstrated that Rb2 had a specific binding affinity for miR-216a and the dissociation constant was 17.6 μM. In both young and senescent human umbilical vein endothelial cells (HUVECs), as well as human aortic endothelial cells, Rb2 decreased the expression of endogenous miR-216a. Next, a replicative endothelial senescence model of HUVECs was established by infection with pre-miR-216a recombinant lentiviruses (Lv-miR-216a) and the number of population-doubling level (PDL) was calculated. Stable overexpression of miR-216a induced a premature senescent-like phenotype, whereas the senescent features and increased activity of senescence-associated β-galactosidase (SA-β-gal) were reversed after Rb2 treatment. The percentage of SA-β-gal-positive cells in senescent PDL25 cells transfected with Lv-miR-216a was decreased 76% by Rb2 treatment compared with the Lv-miR-216a group without Rb2 treatment (P=0.01). Mechanistically, miR-216a inhibited Smad3 protein expression, promoted IκBα degradation and activated NF-κB-responsive genes, such as vascular cell adhesion molecule 1 (VCAM1), which promoted the adhesiveness of endothelial cells to monocytes. These pro-inflammatory effects of miR-216a were significantly suppressed by Rb2 treatment. When Smad3 was suppressed by small interfering RNA, the elevated expression levels of intercellular adhesion molecule 1 and VCAM1 induced by miR-216a were significantly reversed. Collectively, to the best of our knowledge, the present study demonstrated for the first time that Rb2 exerted an anti-inflammation effect on the process of endothelial cell senescence and could be a potential therapeutic drug by targeting miR-216a.

Correspondence to: Professor Weili Zhang or Miss Yu Chen, State Key Laboratory of Cardiovascular Disease, Fuwai Hospital, National Center for Cardiovascular Diseases, Peking Union Medical College and Chinese Academy of Medical Sciences, 167 Beilishi Road, Beijing 100037, P.R. China
E-mail: zhangweili1747@yahoo.com
E-mail: chenyufw@163.com

*Contributed equally

Key words: ginsenoside Rb2, endothelial senescence, microRNA-216a, atherosclerosis

Introduction

Cardiovascular diseases are the primary cause of mortality worldwide, accounting for 31% of all deaths globally in 2016 and it was estimated that 17.9 million people died due to cardiovascular causes (1). Atherosclerosis is regarded as the pathological process that underlies cardiovascular diseases (2). Epidemiological and experimental studies have shown that age-related endothelial dysfunction is a major risk factor for atherosclerosis (3). The vascular endothelium is a thin layer of cells that lines the innermost surface of blood vessels and functions as a semi-selective barrier, which prevents lipid infiltration into the vessel wall (4). Accumulating evidence has suggested the involvement of endothelial cell senescence in endothelial inflammation, which promotes the recruitment of circulating monocytes and contributes to the pathogenesis of

atherosclerosis (5,6). Thus, there is a critical need to identify approaches to protect against endothelial senescence.

MicroRNAs (miRNAs/miRs) are endogenous small single-strand non-coding RNAs of 18-22 nucleotides that serve a major role in the development of atherosclerosis (7,8). Our previous study revealed that miR-216a induced endothelial cell senescence and inflammation via the Smad3/IκBα signaling pathway (9). Moreover, the plasma miR-216a level was elevated in elderly patients with coronary artery disease (9). These findings suggest that miR-216 may be a novel biomarker and therapeutic target of endothelial senescence and atherosclerosis. By using drug-RNA interaction predictor software, the present study examined the potential interaction between chemical molecules and miR-216a on the basis of its sequence and structural features. Here, the present study tested the hypothesis that ginsenoside Rb2 (Rb2), a small chemical molecule, suppresses endothelial senescence mediated by miR-216a.

Rb2, a 20(S)-protopanaxadiol glycoside, is the main bioactive component extracted from the plant *Pannax ginseng*, and is a widely used traditional Chinese medicine (10,11). The molecular formula of Rb2 is $C_{53}H_{90}O_{22}$ and the chemical structure is shown in Fig. S1. The Rb2 has been reported to exert anti-inflammatory effects by upregulating the expression level of G protein-coupled receptor protein 120, a ω-3 fatty acid receptor in monocytes (12). Rb2 also promotes glucose metabolism and attenuates fat accumulation via AKT-dependent signaling mechanisms (13). To date, the effects of Rb2 on endothelial senescence and inflammation remain unknown.

In the present study, considering that cellular senescence and the related inflammatory process are induced by numerous stressors, such as mitochondrial deterioration, oxidative stress, expression of certain oncogenes, DNA damage and chromatin disruption (14), a miR-216a-induced endothelial senescence model was established by transfecting cells with Lv-miR-216a to assess the effect of Rb2 on endothelial senescence and inflammation by acting as a specific inhibitor of the miR-216a/Smad3 pathway, thus aiming to investigate the therapeutic potential of Rb2 in endothelial senescence and atherosclerosis.

Materials and methods

Microscale thermophoresis (MST) assay. A drug-RNA interaction predictor software (rnanut.net/drip) was used to examine the potential interaction between Rb2 and miR-216a on the basis of its sequence and structural features. The MST assay is a biophysical technology for testing interactions between protein and protein or nucleic acid, as well as interactions between nucleic acid and small molecules (15). In the current study, the MST experiment was applied to assess the interaction between Rb2 and miR-216a. The wild-type or mutant-type probe of miR-216a was labeled with 5-carboxyfluorescein (5'FAM), and the sequences were 5'-UAAUCUCAGCUGGCAACUGUGA-3' for wild-type probe, and 5'-UAUAGAGUGCUGGCAACUGUGA-3' for mutant-type probe. Rb2 (purity 98.26%; MedChemExpress) was dissolved in RNase-free water, and then serial doubling dilutions of Rb2 were created from 1 mM to 30 nM for the MST experiment. The 5'FAM-labeled probe of miR-216a (500 nM) and Rb2 dilutions were mixed in a 1:1 ratio and incubated for 5 min at room temperature in the dark. The mixtures were then filled into the capillaries, and the florescence was detected at 400 nm of excitation light wavelength using the Monolith NT.115 MTS instrument (NanoTemper Technologies GmbH). The binding ability between miR-216a and Rb2 was assessed using the dissociation constant (K_d).

Cell culture. The primary human umbilical vein endothelial cells (HUVECs) were isolated from the human umbilical cord veins, as described previously (9,16,17). The umbilical cord samples were donated by 3 healthy pregnant women (aged, 25-30 years) at Beijing Haidian Material & Child Health Hospital (Beijing, China) and collected from January to February, 2020. Informed consent was obtained from the donors. The study was approved by the ethics committee of Fuwai Hospital. The HUVECs were cultured using the endothelial cell medium (ScienCell Research Laboratories, Inc.) supplemented with 1% endothelial cell growth supplement (ScienCell Research Laboratories, Inc.), 5% FBS (ScienCell Research Laboratories, Inc.) and 1% penicillin-streptomycin solution in an incubator with 5% CO_2 at 37˚C.

A replicative senescent model of endothelial cells was established by passaging, and the number of population-doubling level (PDL) was calculated using the equation: $PD=\log_2 (Ch/Cs)$, in which Ch is the number of viable cells at harvest and Cs is the number of cells seeded (6). The PDLs vs. time growth curves were obtained to assess the cellular replication potentiality over time. PDL8 was identified as young HUVECs at a culture of 5-8 days, and PDL44 as senescent cells at a culture of ~75 days. In this study, given the potential difference in the differentiate rate of HUVECs, in order to calculate the PDLs accurately when establishing the replicative senescence model, the HUVECs derived from different donors were not mixed. However, the main experiments were replicated in HUVECs from three independent donors to assess the findings.

Human aortic endothelial cells (HAECs) from a pool of three individuals (lot nos. 11,035, 3,535 and 11,385; cat. no. 6100; ScienCell Research Laboratories, Inc.) were cultured to evaluate the effects of Rb2. HAECs were cultured in the same condition as HUVECs.

Rb2 treatment and miR-216a expression analysis. The PDL8 and PDL44 HUVECs were cultured and grown to 90% confluency, and were then treated with Rb2 at various concentrations of 0.1, 1, 10 and 100 μM for 24 h at 37˚C, in order to investigate the effect of Rb2 on the expression of endogenous miR-216a.

miRNA expression analysis was performed via reverse transcription-quantitative (RT-q)PCR. In brief, the total RNA was extracted from cultured cells using TRIzol® (Invitrogen; Thermo Fisher Scientific, Inc.), and cDNA was reverse transcribed with All-in-One™ miRNA First-Strand cDNA Synthesis kit (GeneCopoeia, Inc) at 37˚C for 15 min and 85˚C for 5 min. Next, the expression of miR-216a was measured by All-in-One™ miRNA qPCR kit (GeneCopoeia, Inc) using an ABI 7500 system (Applied Biosystems; Thermo Fisher Scientific, Inc.). The reaction conditions were as follows: initial denaturation at 94˚C for 10 min, followed by 40 cycles of denaturation at 94˚C for 15 sec, annealing at 55˚C for 1 min

and extension at 72˚C for 10 min. U6 was used as internal reference and the relative gene expression of miR-216a was analyzed using the relative quantification ($2^{-\Delta\Delta Cq}$) method (18). The primer sequences of miR-216a and U6 (GeneCopoeia, Inc.) were as follows: miR-216a-5p 5'-TCTCAGCTGGCAACTGTG AAA-3' and U6 5'-GGTCGGGCAGGAAGAGGGC-3'.

miRNA lentivirus infection. Lentiviruses expressing miR-216a and the negative control (NC) vector were constructed by Shanghai Genechem Co., Ltd. According to the manufacturer's instructions, the coding sequence of pre-miR-216a was inserted into GV369 vector (Ubi-EGFP-MCS-IRES-puromycin) and the construct was verified via DNA sequencing. Next, to collect the lentiviral particles, 293T cells were transfected with 20 μg lentiviral vectors mixed with 1 ml transfection reagent (Genechem Co., Ltd) at 37˚C for 48 h, and cell culture supernatants were harvested 48 h after transfection, centrifuged at 4,000 x g at 4˚C for 10 min and passed through the 0.45 μM filter to remove cellular debris. Finally, lentiviral particles were resolved in PBS and aliquoted for storage at -80˚C as viral stocks.

To establish the stable cell line of miR-216a, HUVECs were infected with pre-miR-216a recombinant lentiviruses (Lv-miR-216a) or NC vectors (Lv-NC) (Shanghai Genechem Co., Ltd.). PDL4 HUVECs were seeded in 24-well cell culture plate (Corning, Inc.) at a density of $5x10^4$ cells/well and added with 5 μl lentiviral vector diluent of $1x10^8$ transducing unit (TU/ml) in each well for a 24-h infection at 37˚C, and then the medium was replaced with fresh growth medium. The multiplicity of infection was 10. After 3 days, cells were treated with 400 ng/ml puromycin (Sigma-Aldrich; Merck KGaA) for selection, and the lentivirus infection efficiency (>95%) was evaluated via the enhanced green fluorescent protein florescence analysis. Then, infected HUVECs were passaged every 3 days and treated with puromycin for selection. PDLs were calculated during the passage. PDL25 cells with stable expression of miR-216a (at ~40 days following Lv-miR-216a infection) were assessed as the senescent cell line and used for subsequent experiments.

miRNA and small interfering (si)RNA transfection. To examine whether Rb2 could affect the target gene expression of miR-216a, PDL8 HUVECs were transfected with miR-216a mimics (Shanghai GenePharma Co., Ltd.) at a final concentration of 50 nM using Lipofectamine® 3000 reagent (Invitrogen; Thermo Fisher Scientific, Inc.). After incubation for 6 h at 37˚C, cells were treated with Rb2 (10 μM) at 37˚C for 48 h and harvested for expression analysis.

To evaluate the effect of Rb2 on the Smad3/IκBα pathway, PDL8 HUVECs were transfected with Smad3 siRNA (si-Smad3; Shanghai GenePharma Co., Ltd.) at a final concentration of 40 nM using Lipofectamine 3000 reagent. After incubation for 6 h at 37˚C, cells were treated with Rb2 (10 μM) at 37˚C for 48 h and then were harvested for expression analysis. The sequences were as follows: miR-216a mimics sense, 5'-UAAUCUCAGCUGGCAACUGUGA-3' and anti-sense, 5'-ACAGUUGCCAGCUGAGAUUAUU-3'; and Smad3 siRNA sense, 5'-AGGACGAGGUCUGCGUGAAUC CCUA-3' and anti-sense, 5'-UAGGGAUUCACGCAGACC UCGUCCU-3'.

Assay for senescence-associated β-galactosidase (SA-β-gal) activity. Endothelial senescence was assessed via *in situ* staining for SA-β-gal positive cells using Senescence β-Galactosidase Staining kit (Beyotime Institute of Biotechnology). β-galactosidase catalyzes the hydrolysis of X-gal, producing a blue color that can be easily visualized under a microscope (19). According to the manufacturer's protocol, cells were treated with fresh β-galactosidase staining solution (pH 6.0) for 16 h at 37˚C without CO_2. The SA-β-gal-positive cells were identified as blue stained cells and images were analyzed using Leica DMI4000 B inverted light microscopes (magnification, x10; Leica Microsystems GmbH). The percentage of SA-β-gal positive-staining cells was calculated by counting five random microscopic fields per sample. The experiment was repeated five times for each group.

Assays for endothelial cell proliferation and adhesion activity. The endothelial proliferative and adhesive abilities were assessed in the senescent PDL25 HUVECs (at ~40 days after transfection of Lv-miR-216a). The cell proliferative ability was assessed using the Cell Counting Kit-8 (CCK-8) method (Beyotime Institute of Biotechnology) according to the manufacturer's instructions. Briefly, HUVECs were seeded into 96-well plate at a density of $5x10^3$ cells/ml and cultured in a 5% CO_2 incubator at 37˚C for 24 h, and were then treated with Rb2 (10 μM) for 24 h at 37˚C. Next, the cells were incubated with 10 μl CCK-8 solution for an additional 1, 2 and 3 h at 37˚C. The absorbance was detected at a wavelength of 450 nm on a LB960 microplate reader (Titertek-Berthold).

The human acute monocytic leukemia cell line (THP-1; China Infrastructure of Cell Line Resources, Beijing, China) was used to assess the endothelial adhesive ability to monocytes. THP-1 cells were labeled with CellTracker™ CM-Dil (red fluorescence; Invitrogen; Thermo Fisher Scientific, Inc.) for 30 min at 37˚C, washed twice with PBS and then were re-suspended in RPMI-1640 medium (Sigma-Aldrich; Merck KGaA) at a density of $1x10^6$ cells/ml. The CM-Dil labeled THP-1 cells were incubated with PDL25 HUVECs at 37˚C for 30 min in an incubator containing 5% CO_2. The non-adherent THP-1 cells were removed by PBS, and the adherent cells were fixed with 4% paraformaldehyde (Beijing Leagene Biotechnology Co., Ltd.) at room temperature for 15 min. The nuclei of cells were stained with DAPI (OriGene Technologies, Inc.) at room temperature for 20 min, and the number of adhesive THP-1 cells to endothelial cells was observed and imaged in five random fields at wavelengths of 359 and 549 nm using a confocal laser scanning microscope (magnification, x20) SP8 (Leica Microsystems GmbH). The experiments were repeated five times.

mRNA expression analysis. The mRNA expression levels of p53, p21, vascular cell adhesion molecule 1 (VCAM1), intercellular adhesion molecule (ICAM1) and Smad3 were analyzed via RT-qPCR (primer sequences are listed in Table SI). Briefly, total RNA was extracted from cells using TRIzol® reagent (Invitrogen; Thermo Fisher Scientific, Inc.). cDNA was reverse transcribed using PrimeScript™ RT Master Mix (Takara Bio, Inc.) under the following thermocycling conditions: 37˚C for 15 min, 85˚C for 5 sec. RT-qPCR was performed using SYBR Green qPCR mix (Shanghai Yeasen Biotechnology Co., Ltd.) on an ABI 7500 system (Applied

Biosystems; Thermo Fisher Scientific, Inc.). The reaction conditions were conducted as following: Initial denaturation for 10 min at 95˚C, followed by 40 cycles of denaturation at 95˚C for 15 sec, annealing and elongation at 60˚C for 1 min, and final extension at 72˚C for 1 min. GAPDH expression was used as internal control, and the expression of target gene was calculated using relative quantification ($2^{-\Delta\Delta Cq}$) method (18).

Western blot analysis. Protein expression levels were determined via western blot analysis. In brief, HUVECs were harvested and proteins extracts were isolated with ice-cold RIPA lysis buffer (Beyotime Institute of Biotechnology) containing protease inhibitor (Roche Diagnostics GmbH). The total concentration of protein was determined using a Pierce BCA Protein Assay kit (Invitrogen; Thermo Fisher Scientific, Inc.). Each sample protein was loaded at 20 μg and separated by 10% SDS-PAGE, and then transferred to nitrocellulose membranes (EMD Millipore). Subsequently, the membrane was blocked with 10% non-fat milk at room temperature for 2 h and then incubated with primary antibodies overnight at 4˚C. The primary antibodies were purchased from Cell Signaling Technology, Inc., including the anti-p53 (1:1,000; cat. no. 2527T), anti-$p21^{Waf1/Cip1}$ (1:1,000; cat. no. 2947T), anti-ICAM1 (1:1,000; cat. no. 67836T), anti-VCAM1 (1:1,000; cat. no. 39036S), anti-Smad3 (1:1,000; cat. no. 9523T) and anti-IκBα (1:1,000; cat. no. 4812S). The mouse monoclonal anti-GAPDH antibody (1:2,000; cat. no. TA309157; OriGene Technologies, Inc.) was applied as an internal control. Then, membranes were incubated with HRP-conjugated anti-rabbit IgG secondary antibody (1:5,000; cat. no. 7074; Cell Signaling Technology, Inc.) or anti-mouse IgG secondary antibody (1:2,000; ZB2305; OriGene Technologies, Inc.) for 1.5 h at room temperature. Bands were visualized with FluorChem R, M and E Systems (ProteinSimple) and analyzed using ImageJ software (v1.5.1; National Institutes of Health).

Statistical analysis. Data are presented as the mean ± SD. For the comparison between two groups, group differences were analyzed compared using an unpaired Student t-test. For the comparisons ≥3 groups, group differences were analyzed using one-way ANOVA with Tukey's post hoc test. Each experiment was repeated ≥3 times independently. Data were analyzed using SPSS 19.0 software (IBM Corp.). P<0.05 was considered to indicate a statistically significant difference.

Results

Binding ability between Rb2 and miR-216a. The bioinformatics analysis with drug-RNA interaction predictor software (rnanut.net/drip) suggested that Rb2 may have a high affinity with miR-216a. In the subsequent MST experiment for assessing the interaction between Rb2 and miR-216a, the results demonstrated that Rb2 bound to the wild-type probe of miR-216a and the K_d value was 17.6 μM (Fig. 1A). By contrast, if the seed sequence of miR-216a was mutated, Rb2 was not detected to bind the mutant-type probe (Fig. 1B), indicating that Rb2 can bind to miR-216a specifically.

Establishment of the senescent HUVECs model. A premature senescent model of endothelial cells induced by miR-216a

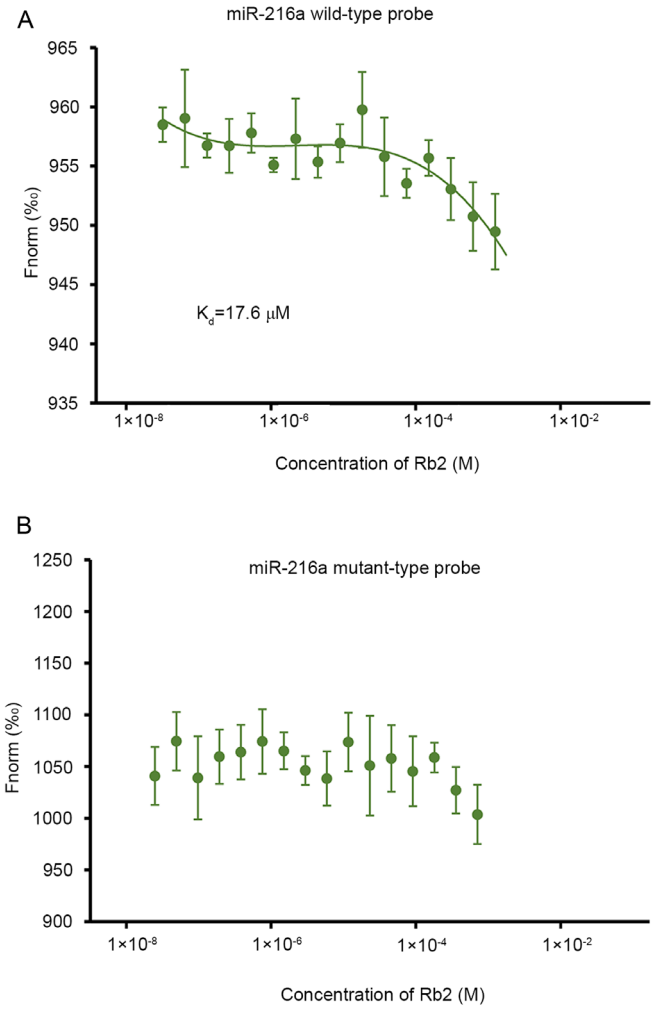

Figure 1. Specific binding affinity between Rb2 and miR-216a. The interaction between Rb2 and miR-216a was examined using the microscale thermophoresis assay *in vitro*, and the binding ability was assessed using the value of the K_d. Fnorm was represented as the ligand-dependent changes in normalized fluorescence. Fnorm is defined as $Fnorm=F_{(hot)}/F_{(cold)}$, where $F_{(hot)}$ and $F_{(cold)}$ represent averaged fluorescence intensities at defined time points of the MST traces. Fnorm is applied to determine the binding constants between Rb2 and miR-216a. (A) High binding ability between Rb2 and the miR-216a wild-type probe. (B) No binding was observed between Rb2 and the miR-216a mutant-type probe. miR-216a, microRNA-216a; K_d, dissociation constant; Rb2, ginsenoside Rb2.

was established. The PDLs-vs.-time growth curves indicated that, in the PDL25 line at ~40 days after transfection with Lv-miR-216a, the cells showed senescent features, characterized by enlarged size and flattened morphology (Fig. 2A), as well as accumulation of SA-β-gal within cytoplasm (blue staining; Fig. 2B), which was similar as the senescent status of naturally passaged PDL44 (at a culture of ~75 days). The percentage of SA-β-gal-positive cells was markedly increased by 130% in the PDL25 line transfected with Lv-miR-216a compared with the NC (P=0.01; Fig. 2C). Moreover, the mRNA expression levels of the senescent-related cell cycle inhibitors p21 and p53 were upregulated by 34% (P=0.05) and 38% (P=0.02; Fig. 2D), respectively; further protein expression analysis also showed that p21 (P=0.05) and p53 (P<0.01) were significantly upregulated (Fig. 2E).

To verify whether pre-miR-216a recombinant lentiviruses were successfully transfected in HUVECs, miR-216a

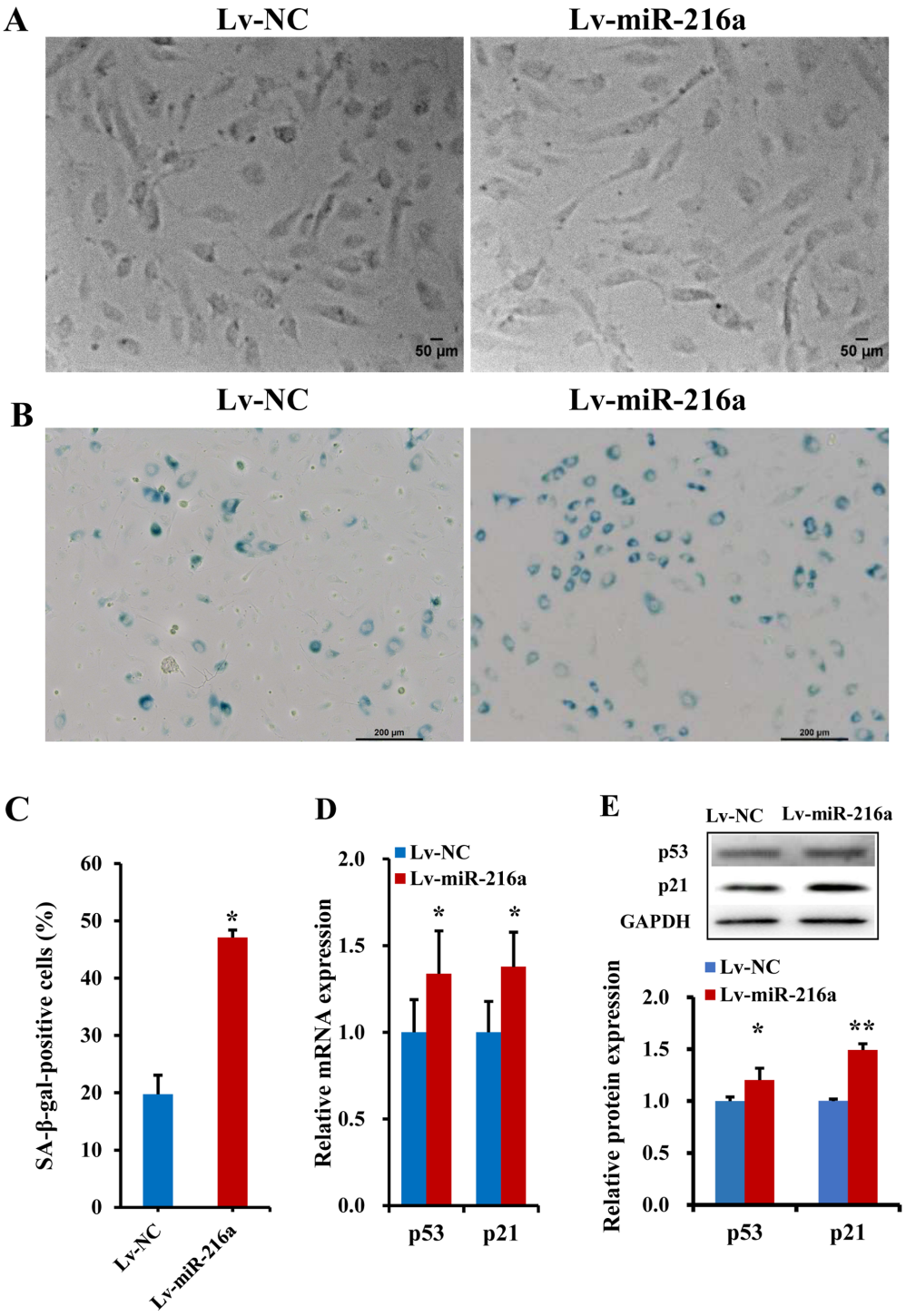

Figure 2. Establishment of a premature senescence phenotype in endothelial cells induced by miR-216a. (A) Images of senescent phenotype, characterized by enlarged size and flattened morphology, in the PDL25 endothelial cell line transfected with Lv-miR-216a compared with cells transfected with Lv-NC vector (n=5). Scale bar, 50 μm. (B) Micrographs of senescent cells, characterized by accumulation of SA-β-gal within cytoplasm (blue staining) in PDL25 cells transfected with Lv-miR-216a compared with the Lv-NC (n=5). Scale bar, 200 μm. (C) Comparisons of the percentage of SA-β-gal-positive cells (of the total cell number) between PDL25 cells transfected with the Lv-miR-216a and the Lv-NC (n=5). (D) mRNA expression levels of senescent-related genes p53 and p21 (n=5). (E) Protein expression levels of senescent-related genes p53 and p21 (n=5). The data are presented as the mean ± SD. *P<0.05, **P<0.01, vs. Lv-NC. miR-216a, microRNA-216a; Lv-miR-216a, pre-miR-216a recombinant lentiviruses; NC, negative control; SA-β-gal, senescence-associated β-galactosidase.

expression was examined using RT-qPCR. Compared with NC (Lv-NC), the expression level of miR-216a in the Lv-miR-216a cell line was increased by 6900% (P<0.01; Fig. S2).

Rb2 attenuates endothelial senescence induced by miR-216a. Serial concentrations of Rb2 were applied to examine the effects of Rb2 on endogenous miR-216a expression. In young PDL8 HUVECs, Rb2 treatment with concentrations of 1, 10 or 100 μM significantly decreased miR-216a expression by 40% (P=0.01), 30% (P=0.02) and 36% (P=0.02), respectively (Fig. 3A). Moreover, in senescent PDL44 HUVECs, Rb2 did not appear to affect miR-216a expression at low doses, whereas a

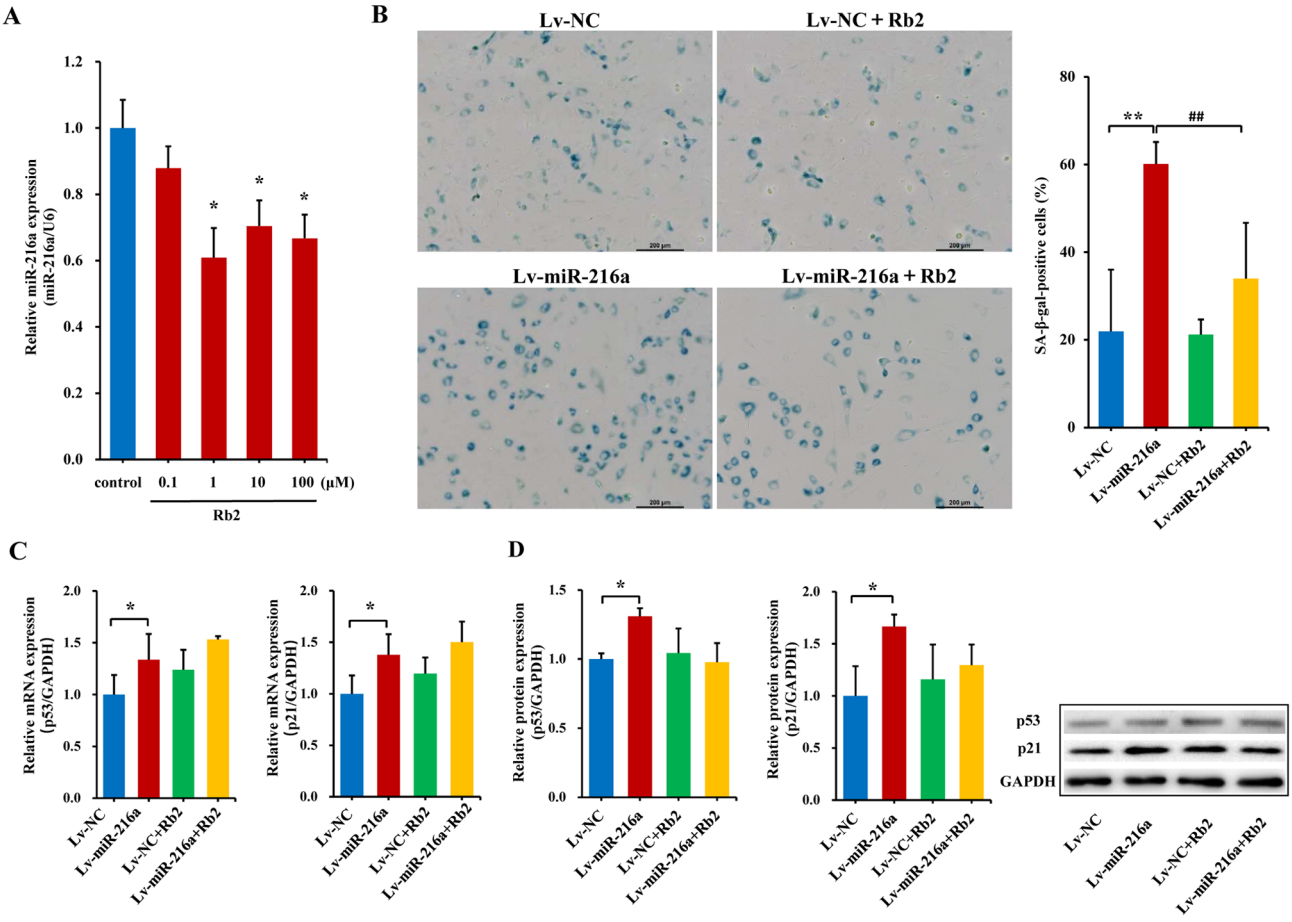

Figure 3. Rb2 attenuates endothelial senescence induced by miR-216a. (A) Serial concentrations of Rb2 were applied to examine the effects of Rb2 on endogenous miR-216a expression in PDL8 HUVECs. *P<0.05, vs. Control. (B) Micrographs of senescent cells characterized by accumulation of SA-β-gal within cytoplasm (blue staining), and comparisons of the SA-β-gal-positive cells in PDL25 cells with Lv-miR-216a transfection after treatment with or without 10 μM Rb2 (n=5). Scale bar, 200 μm. (C) mRNA expression levels of senescent-related genes p53 and p21 in PDL25 cells transfected with Lv-miR-216a with or without Rb2 treatment (n=5). (D) Protein expression levels of senescent-related genes p53 and p21 in PDL25 cells transfected with Lv-miR-216a with or without Rb2 treatment (n=5). Data are presented as the mean ± SD. *P<0.05, **P<0.01; ##P<0.01. miR-216a, microRNA-216a; Lv-miR-216a, pre-miR-216a recombinant lentiviruses; NC, negative control; SA-β-gal, senescence-associated β-galactosidase; Rb2, ginsenoside Rb2.

relative high dose (100 μM) of Rb2 exerted a significant inhibitory effect on miR-216a expression by 44% (P=0.01; Fig. S3), supporting the previous finding that endogenous miR-216a was highly expressed in senescent endothelial cells (9). However, the concentration of 100 μM Rb2 has previously been shown to induce cytotoxic effects on endothelial cells (20). In HAECs, Rb2 (10 μM) also decreased the expression level of endogenous miR-216a by 34% (P=0.02; Fig. S4). Given that the K_d value was 17.6 μM in the MST experiment assessing the special binding ability between Rb2 and miR-216a, the concentration of 10 μM of Rb2 was selected as the optimal dose and used in further experiments.

Next, the potential role of Rb2 in endothelial senescence and dysfunctions induced by miR-216a was assessed. In the premature senescent model of PDL25 HUVECs with Lv-miR-216a transfection, the percentage of SA-β-gal-positive cells were increased by 174% (P<0.01; Fig. 3B) compared with the Lv-NC; whereas the senescent features and accumulation of SA-β-gal within cytoplasm induced by miR-216a were reversed following Rb2 treatment, and the percentage of SA-β-gal-positive cells decreased by 76% in the Lv-miR-216a+Rb2 group compared with the Lv-miR-216a group (P<0.01; Fig. 3B). The elevated mRNA and protein expression levels of p53 (P=0.05) and p21 (P=0.04) induced by miR-216a were not significantly affected by Rb2 treatment (Fig. 3C and D).

Rb2 inhibits the adhesiveness of endothelial cells to monocytes induced by miR-216a. In senescent PDL25 HUVECs with overexpression of miR-216a, the adhesive ability of endothelial cells (DAPI-staining) to THP-1 cells (CM-Dil-staining) was increased by 180% compared with the NC (P<0.01), whereas this promoting effect of miR-216a was significantly inhibited by Rb2 treatment (P<0.01; Fig. 4A and B). Consistently, the mRNA expression level of adhesion cytokine VCAM1 was upregulated by 78% by Lv-miR-216a (P=0.02), while this effect was inhibited by Rb2 (P=0.04; Fig. 4C), and these effects were also observed via further protein expression analysis (both P<0.05; Fig. 4D). Additionally, the proliferative ability of endothelial cells was examined in senescent PDL25 cells, and the inhibitory effect of miR-216a was not affected by Rb2 (Fig. S5).

Rb2 reverses the inhibitory role of miR-216a on the expression of the Smad3/IκBa pathway. Our previous study has

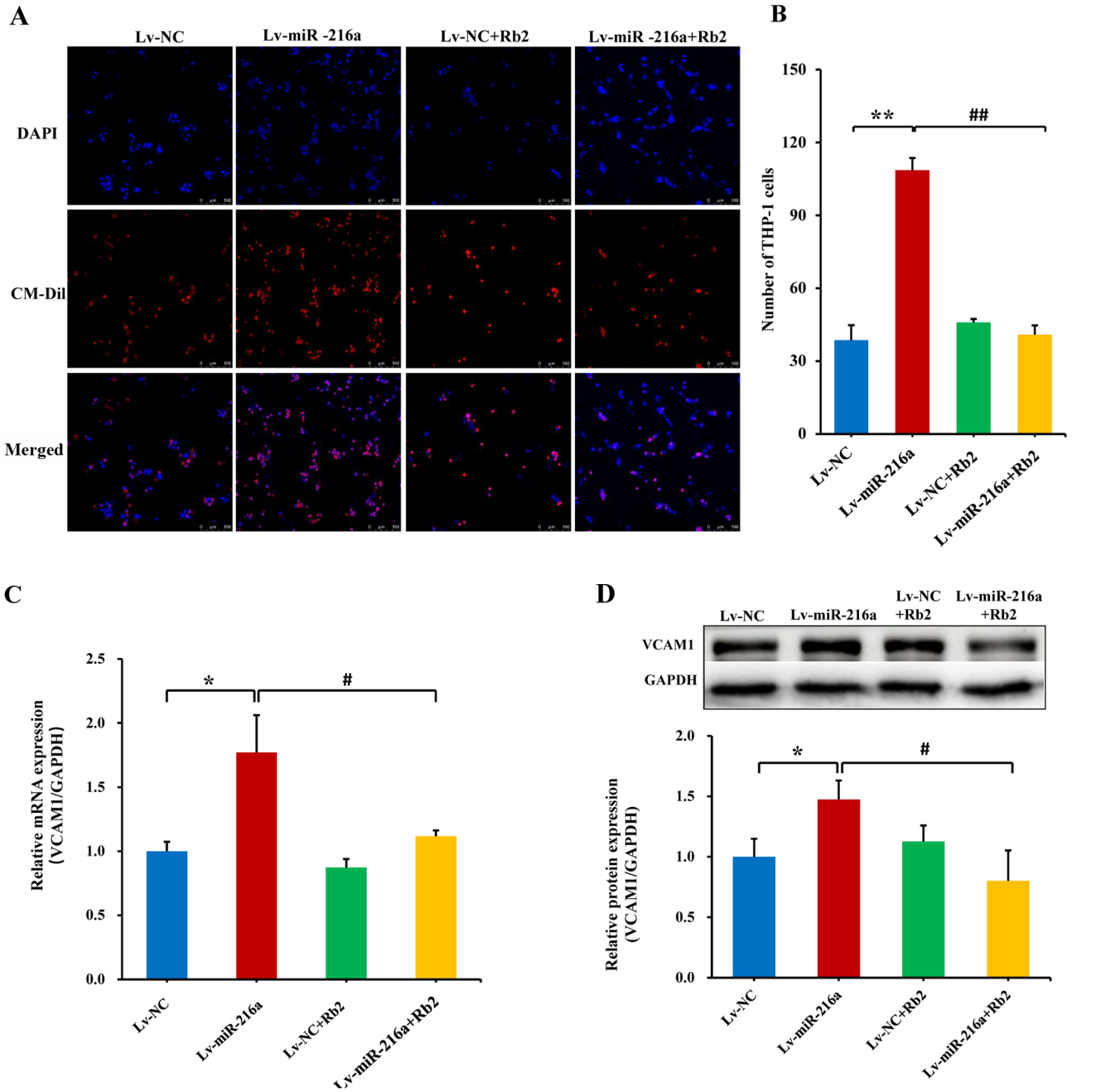

Figure 4. Rb2 inhibits the adhesiveness of endothelial cells to monocytes induced by miR-216a. (A) Images of THP-1 cells adhering to PDL25 HUVECs with stable miR-216a expression after treatment with 10 μM Rb2. DAPI-staining (blue fluorescence) was used to label the nuclei of HUVECs and THP-1 cells, and CM-Dil (red fluorescence) was used to label THP-1 cells specifically. Scale bar, 100 μm. (B) Comparisons of the number of adhesive THP-1 cells with or without Rb2 treatment (n=5). (C) mRNA expression level of the adhesion molecule VCAM1 with or without Rb2 treatment (n=5). (D) Protein expression level of the adhesion molecule VCAM1 with or without Rb2 treatment (n=5). *P<0.05, **P<0.01; $^{\#}$P<0.05, $^{\#\#}$P<0.01. miR-216a, microRNA-216a; Lv-miR-216a, pre-miR-216a recombinant lentiviruses; NC, negative control; VCAM1, vascular cell adhesion molecule 1; Rb2, ginsenoside Rb2.

shown that miR-216a can directly inhibit the Smad3/IκBα signaling pathway, and therefore, promote the endothelial inflammatory process (6). Thus, the current study transfected miR-216a mimics in PDL8 HUVECs to observe the effect of miR-216a on the protein expression levels of Smad3 and IκBα. To verify whether miR-216a mimics was successfully transfected, miR-216a expression was examined using RT-qPCR. Compared with the NC group, the expression level of miR-216a was increased by 422-fold (P<0.01; (Fig. S6). The results consistently demonstrated that miR-216a decreased the protein expression levels of Smad3 and IκBα (P<0.01) in PDL8 HUVECs transfected with miR-216a mimics, and the role of miR-216a was significantly reversed by Rb2 treatment (P<0.01; Fig. 5A).

To further assess whether Rb2 reversed the role of endogenous miR-216a in the Smad3/IκBa pathway, Smad3 siRNA was transfected to PDL8 HUVECs. As expected, the mRNA and protein expression levels of Smad3 were greatly decreased by silencing Smad3 (P<0.01; Fig. 5B), and consequently the mRNA and protein expression levels of downstream adhesion molecules ICAM1 and VCAM1 were upregulated (both P<0.05; Fig. 5C). By contrast, when exposed to Rb2, the expression

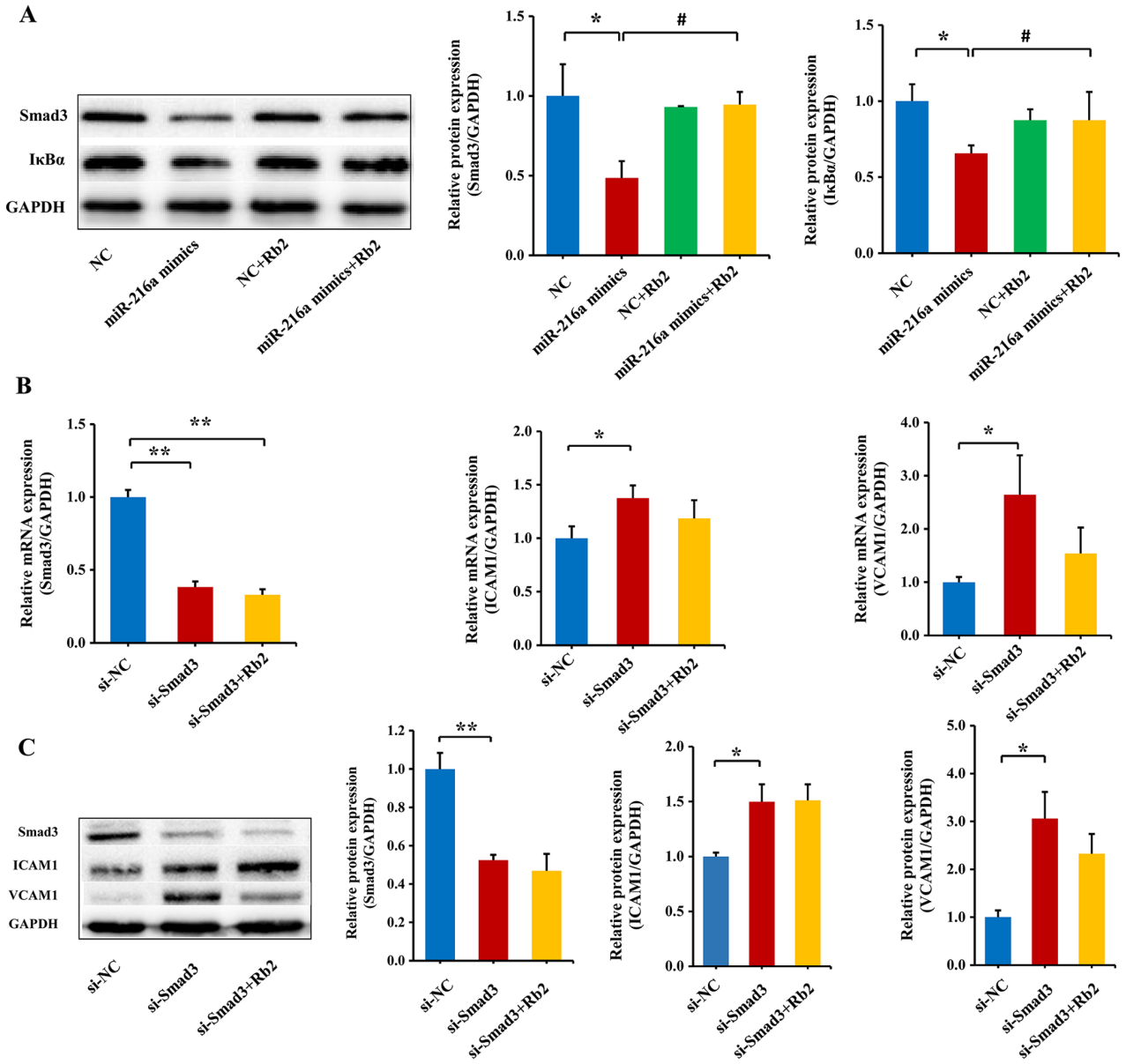

Figure 5. Rb2 reverses the effect of miR-216a on the Smad3/IκBa signaling pathway. (A) Protein expression levels of Smad3 and IκBα with or without Rb2 treatment in PDL8 HUVECs transfected with miR-216a mimics (n=5). *P<0.05; $^{\#}$P<0.05. (B) mRNA expression levels of Smad3, ICAM1 and VCAM1 after silencing Smad3 in PDL8 HUVECs with or without Rb2 treatment (n=5). (C) Protein expression levels of Smad3, ICAM1 and VCAM1 after silencing Smad3 in PDL8 HUVECs with or without Rb2 treatment (n=5). *P<0.05, **P<0.01. miR-216a, microRNA-216a; NC, negative control; VCAM1, vascular cell adhesion molecule 1; Rb2, ginsenoside Rb2; ICAM1, intercellular adhesion molecule; si, small interfering RNA.

levels of ICAM1 and VCAM1 were reversed, although the findings were not significant (Fig. 5C). These results suggested that Rb2 attenuated the inflammatory process by inhibiting the expression level of Smad3 targeted by miR-216a.

Discussion

To the best of our knowledge, the present study demonstrated the first time that Rb2 had a specific affinity for miR-216a, and further experiments identified that Rb2 attenuated endothelial senescence and the adhesiveness of monocytes to senescent HUVECs induced by miR-216a. Moreover, miR-216a promoted the endothelial inflammatory process by inhibiting the Smad3 and IκBα signaling pathway, and the role of miR-216a was suppressed after Rb2 treatment. These findings indicated that Rb2 may serve as a potential therapeutic drug for endothelial cell senescence and inflammation by targeting miR-216a.

Atherosclerosis, an aging-related, chronic inflammatory process, is accelerated by endothelial senescence and dysfunction (21,22). In our previous study, it was found that miR-216a promoted endothelial senescence and inflammation by inhibiting the Smad3/IκBα pathway, and notably, elderly patients with coronary artery disease had an elevated concentrations of plasma miR-216a, all of which indicate that miR-216a may be a therapeutic target (9).

miRNAs are emerging as an appealing target for drug discovery, the these traditionally include oligonucleotides that are complementary to a miRNA and block its activity, as well as duplex or chemically-modified single-stranded RNAs that mimic a miRNA and trigger enhanced activity (23,24). For

example, 2'-F- and 2'-MOE-modified anti-miR-33 has been shown to reduce atherosclerosis in non-human primates (25). Moreover, the mimics of miR-34 represses oncogene expression and blocks tumor growth (26), while single-stranded oligonucleotides complementary to miR-122 have been developed to treat hepatitis C virus (27). However, there are some drawbacks, such as unwanted exogenous RNA immunogenicity, poor stability, weak cell permeability and high costs (28). Preclinical and clinical studies have also showed that delivery of miRNAs-based chemistries has side effects and may lead to off-target effects (29,30).

Recently, targeting miRNAs using chemical small molecules has become a promising strategy for disease treatment (31). In the present study, bioinformatics analysis and validating experiments identified that Rb2 bound to miR-216a specifically and inhibited the expression level of endogenous miR-216a in endothelial cells. However, the inhibitory effect of Rb2 on miR-216a appeared not to occur in a dose-dependent manner. There are some explanations for these results as follows: First, the mode of Rb2 binding to miR-216a remains to be fully elucidated. Drug-RNA interaction predictor software was used to predict that Rb2 had a high binding score for miR-216a by identifying cleft and pocket-containing motifs in the primary sequence and secondary structural elements of miR-216a. The binding model of RNA motif-Rb2 pairs may cause a conformational change in miR-216a and influence its RNA binding activity. Of note, miRNAs can fold into structural composites including base-paired and non-canonically paired regions with three dimensional structures. Thus, the direct interactions between miRNAs and small molecules are complex, including cross-linking and cleavage to alter the miRNA sequence and recruit nucleases (32,33). However, approaches remain to be established to identify compound modules or fragments that selectively bind miRNA motifs, and to define factors that influence the bioactivities of small chemical molecules and miRNAs.

It is reasonable to suggest that the intracellular microenvironment may affect the inhibitory manner of ginsenosides on miRNA expression in various cell types. Previous studies have reported that several types of ginsenosides show a dose-dependent effect on expression levels of targeted miRNAs, whereas others have not (34-36). For example, notoginsenoside R1 markedly suppresses miR-301a expression in murine chondroprogenitor cells at a relatively high concentration, but does not influence miR-301a expression at a low dose (34). It has also been shown that ginsenoside Rg1 reduced miR-148-5p expression in rat bone marrow mesenchymal stem cells and that ginsenoside Rg3 that downregulated miR-221 expression in human oral squamous carcinoma cells; however, the inhibitory effects of ginsenosides were not in a dose-dependent manner (35,36). In the current study, various concentrations (1, 10 or 100 μM) of Rb2 significantly decreased the expression level of endogenous miR-216a in young PDL8 HUVECs, whereas only a relative high dose (100 μM) of Rb2 had an inhibitory effect on miR-216a in PDL44 cells, which supports our previous finding that endogenous miR-216a was highly expressed in senescent endothelial cells compared with younger cells (9).

The present study also evaluated the inhibitory effect of Rb2 on miR-216a in arterial endothelial cells, and found that Rb2 significantly decreased expression of endogenous miR-216a in HAECs. However, transfection of miR-216a into HAECs induced the phenotype of endothelial-mesenchymal transition (EnMT) in an early cell passage. There are several explanations for this finding. For instance, HAECs isolated from human adult arteries are highly differentiated cells, and may have a different mechanism during endothelial aging implicated in atherosclerosis (37,38). Moreover, there may be differences in characteristics and functions between arteries and venous endothelial cells (39,40). Fleenor *et al* (41) also observed that a model of primary human cell aging induced EnMT in an early passage of HAECs, which was similar to the phenotype observed in late passage cells. HAECs and HUVECs may react differently to aging and inflammation induced by miR-216a, and therefore, more comprehensive experiments are required to further evaluate the complex effects of Rb2 and miR-216a in vascular biology, considering the biological difference in vascular endothelial cells.

Rb2 is one of the most highly abundant components in ginseng, and has been reported to possess various bioactivities including anti-inflammatory, anti-oxidative and anti-tumor effects (12,13). The present study first investigated the inhibitory effect of Rb2 on endothelial senescence and the inflammatory process induced by miR-216a. Smad3 is a direct target gene of miR-216a (9). The present study found that miR-216a inhibited Smad3 protein expression, promoted downstream IκBα degradation, and thus, activated NF-κB responsive genes, such as VCAM1, which promoted the adhesiveness of endothelial cells to monocytes. The inhibitory effect of miR-216a on Smad3 and IκBα expression was reversed by Rb2 treatment, which indicated that Rb2 may exert an anti-inflammation effect, thereby acting as a potential therapeutic drug for endothelial cell senescence and inflammation by targeting miR-216a.

Of note, the present study identified that miR-216a inhibited the proliferative ability of endothelial cells, but the inhibitory effect of miR-216a was not attenuated by Rb2. Additionally, expression levels of p53 and p21 genes were not significantly affected by Rb2. These results are consistent with the characteristics of senescent cells, such as a flattened and enlarged cell morphology and growth arrest, which may lead to irreversible impairment of proliferative ability of endothelial cells (42). Aging-related genes p53 and p21 serve an important role in cell-cycle control, DNA repair and cellular stress responses, and their expression gradually increases during the process of replicative senescence (43). Thus, it was suggested that Rb2 attenuated the endothelial senescence mainly via the inflammatory process induced by miR-216a, although the underlying mechanism should be clarified further.

In conclusion, the present study demonstrated that Rb2 had a specific binding affinity for miR-216a, and further attenuated the senescent status and inflammatory process induced by miR-216a via the Smad3/IκBα signaling pathway. These data indicated that Rb2 may exert an anti-inflammatory effect on the process of endothelial cell senescence, acting as a potential therapeutic drug by targeting miR-216a.

Acknowledgements

Not applicable.

Funding

This work was supported by the grants from National Natural Science Foundation of China (grant nos. 81873492 and 81670338) and from State Key Laboratory of Cardiovascular Disease at Fuwai Hospital (grant no. 2019kf-03).

Availability of data and materials

The datasets used and/or analyzed during the current study are available from the corresponding author on reasonable request.

Authors' contributions

All authors contributed to the study conception and design. Material preparation, data collection and analysis were performed by YTC, SW, SY, RL and YY. The authenticity of raw data was assessed and confirmed by YTC, SW, YC and WZ. The draft of the manuscript was written by YTC, YC and WZ. All authors read and approved the final manuscript.

Ethics approval and consent to participate

The present study was approved by Ethics Committee of Fuwai Hospital, and informed consent was obtained from the healthy donor.

Patient consent for publication

Not applicable.

Competing interests

The author declare that they have no competing interests.

References

1. Evans MA, Sano S and Walsh K: Cardiovascular disease, aging, and clonal hematopoiesis. Annu Rev Pathol 15: 419-438, 2020.
2. Schaftenaar F, Frodermann V, Kuiper J and Lutgens E: Atherosclerosis: The interplay between lipids and immune cells. Curr Opin Lipidol 27: 209-215, 2016.
3. Libby P, Ridker PM and Hansson GK: Progress and challenges in translating the biology of atherosclerosis. Nature 473: 317-325, 2011.
4. Ghosh A, Gao L, Thakur A, Siu PM and Lai CWK: Role of free fatty acids in endothelial dysfunction. J Biomed Sci 24: 50, 2017.
5. Menghini R, Stöhr R and Federici M: MicroRNAs in vascular aging and atherosclerosis. Ageing Res Rev 17: 68-78, 2014.
6. Childs BG, Gluscevic M, Baker DJ, Laberge RM, Marquess D, Dananberg J and van Deursen JM: Senescent cells: An emerging target for diseases of aging. Nat Rev Drug Discov 16: 718-735, 2017.
7. Feinberg MW and Moore KJ: MicroRNA regulation of atherosclerosis. Circ Res 118: 703-720, 2016.
8. Lu Y, Thavarajah T, Gu W, Cai J and Xu Q: Impact of miRNA of atherosclerosis. Arterioscler Thromb Vasc Biol 38: e159-e170, 2018.
9. Yang S, Mi X, Chen Y, Feng C, Hou Z, Hui R and Zhang W: MicroRNA-216a induces endothelial senescence and inflammation via Smad3/IκBα pathway. J Cell Mole Med 22: 2739-2749, 2018.
10. Hasegawa H: Proof of the mysterious efficacy of ginseng: Basic and clinical trials: Metabolic activation of ginsenoside: Deglycosylation by intestinal bacteria and esterification with fatty acid. J Pharmacol Sci 95: 153-157, 2004.
11. Zhang Y, Han LF, Sakah KJ, Wu ZZ, Liu LL, Agyemang K, Gao XM and Wang T: Bioactive protopanaxatriol type saponins isolated from the roots of Panax notoginseng (Burk.) F. H. Chen. Molecules 18: 10352-10366, 2013.
12. Huang Q, Wang T and Wang HY: Ginsenoside Rb2 enhances the anti-inflammatory effect of ω-3 fatty acid in LPS-stimulated RAW264.7 macrophages by upregulating GPR120 Expression. Acta Pharmacol Sin 38: 192-200, 2017.
13. Dai S, Hong Y, Xu J, Lin Y, Si Q and Gu X: Ginsenoside Rb2 promotes glucose metabolism and attenuates fat accumulation via AKT-dependent mechanisms. Biomed Pharmacother 100: 93-100, 2018.
14. Childs BG, Durik M, Baker DJ and van Deursen JM: Cellular senescence in aging and age-related disease: From mechanisms to therapy. Nat Med 21: 1424-1435, 2015.
15. Wienken CJ, Baaske P, Rothbauer U, Braun D and Duhr S: Protein-binding assays in biological liquids using microscale thermophoresis. Nat Commun 19: 100, 2010.
16. Jaffe EA, Nachman RL, Becker CG and Minick CR: Culture of human endothelial cells derived from umbilical veins. Identification by morphologic and immunologic criteria. J Clin Invest 52: 2745-2756, 1973.
17. Ma L, Li G, Cao G, Zhu Y, Du MR, Zhao Y, Wang H, Liu Y, Yang Y, Li YX, *et al*: dNK cells facilitate the interaction between trophoblastic and endothelial cells via VEGF-C and HGF. Immunol Cell Biol 95: 695-704, 2017.
18. Livak KJ and Schmittgen TD: Analysis of relative gene expression data using real-time quantitative PCR and the 2(-Delta Delta C(T)) method. Methods 25: 402-408, 2001.
19. Dimri GP, Lee X, Basile G, Acosta M, Scott G, Roskelley C, Medrano EE, Linskens M, Rubelj I, Pereira-Smith O, *et al*: A biomarker that identifies senescent human cells in culture and in aging skin in vivo. Proc Natl Acad Sci USA 92: 9363-9367, 1995.
20. Liu JW, Wei DZ, Du CB and Zhong JJ: Enhancement of fibrinolytic activity of bovine aortic endothelial cells by ginsenoside Rb2. Acta Pharmacol Sin 24: 102-108, 2003
21. Minamino T, Miyauchi H, Yoshida T, Ishida Y, Yoshida H and Komuro I: Endothelial cell senescence in human atherosclerosis: Role of telomere in endothelial dysfunction. Circulation 105: 1541-1544, 2002.
22. Gimbrone MA Jr and García-Cardeña G: Endothelial cell dysfunction and the pathobiology of atherosclerosis. Circ Res 118: 620-636, 2016.
23. Ling H, Fabbri M and Calin GA: MicroRNAs and other non-coding RNAs as targets for anticancer drug development. Nat Rev Drug Discov 12: 847-865, 2013.
24. Dangwal S and Thum T: MicroRNA therapeutics in cardiovascular disease models. Annu Rev Pharmacol Toxicol 54: 185-203, 2014.
25. Rayner KJ, Esau CC, Hussain FN, McDaniel AL, Marshall SM, van Gils JM, Ray TD, Sheedy FJ, Goedeke L, Liu X, *et al*: Inhibition of miR-33a/b in non-human primates raises plasma HDL and lowers VLDL triglycerides. Nature 478: 404-407, 2011.
26. Agostini M and Knight RA: miR-34: From bench to bedside. Oncotarget 5: 872-881, 2014.
27. Thakral S and Ghoshal K: miR-122 is a unique molecule with great potential in the diagnosis, prognosis of liver disease and therapy both as miRNA mimic and antimir. Curr Gene Ther 15: 142-150, 2015.
28. Matsui M and Corey DR: Non-coding RNAs as drug targets. Nat Rev Drug Discov 16: 167-179, 2017.
29. van Rooij E and Olson EN: MicroRNA therapeutics for cardiovascular disease: Opportunities and obstacles. Nat Rev Drug Discov 11: 860-872, 2012.
30. McClorey G and Wood MJ: An overview of the clinical application of antisense oligonucleotides for RNA-targeting therapies. Curr Opin in Pharmacol 24: 52-58, 2015.
31. Fan R, Xiao C, Wan X, Cha W, Miao Y, Zhou Y, Qin C, Cui T, Su F and Shan X: Small molecules with big roles in microRNA chemical biology and microRNA-targeted therapeutics. RNA Biol 16: 707-718, 2019.
32. Warner KD, Hajdin CE and Weeks KM: Principles for targeting RNA with drug-like small molecules. Nat Rev Drug Discov 17: 547-558, 2018.
33. Disney MD: Targeting RNA with small molecules to capture opportunities at the intersection of chemistry, biology, and medicine. J Am Chem Soc 141: 6776-6790, 2019.
34. Dong Y, Yan X, Yang X, Yu C, Deng Y, Song X and Zhang L: Notoginsenoside R1 suppresses miR-301a via NF-κB pathway in lipopolysaccharide-treated ATDC5 cells. Exp Mol Pathol 112: 104355, 2020.
35. Zheng HZ, Fu XK, Shang JL, Lu RX, Ou YF and Chen CL: Ginsenoside Rg1 protects rat bone marrow mesenchymal stem cells against ischemia induced apoptosis through miR-494-3p and ROCK-1. Eur J Pharmacol 822: 154-167, 2018.

36. Cheng Z and Xing D: Ginsenoside Rg3 inhibits growth and epithelial-mesenchymal transition of human oral squamous carcinoma cells by down-regulating miR-221. Eur J Pharmacol 853: 353-363, 2019.
37. Rippe C, Blimline M, Magerko KA, Lawson BR, LaRocca TJ, Donato AJ and Seals DR: MicroRNA changes in human arterial endothelial cells with senescence: Relation to apoptosis, eNOS and inflammation. Exp Gerontol 47: 45-51, 2012.
38. Xiong Y, Yepuri G, Forbiteh M, Yu Y, Montani JP, Yang Z and Ming XF: ARG2 impairs endothelial autophagy through regulation of MTOR and PRKAA/AMPK signaling in advanced atherosclerosis. Autophagy 10: 2223-2238, 2014.
39. Dela Paz NG and D'Amore PA: Arterial vs. venous endothelial cells. Cell Tissue Res 335: 5-16, 2009.
40. Hirashima M and Suda T: Differentiation of arterial and venous endothelial cells and vascular morphogenesis. Endothelium 13: 137-145, 2006.
41. Fleenor BS, Marshall KD, Rippe C and Seals DR: Replicative aging induces endothelial to mesenchymal transition in human aortic endothelial cells: Potential role of inflammation. J Vasc Res 49: 59-64, 2012.
42. Kaur J and Farr JN: Cellular senescence in age-related disorders. Transl Res 226: 96-104, 2020.
43. Rufini A, Tucci P, Celardo I and Melino G: Senescence and aging: The critical roles of p53. Oncogene 32: 5129-5143, 2013.